EFFECTS OF MAGNESIUM AND CHLORIDE IONS ON LIMESTONE DUAL ALKALI SYSTEM PERFORMANCE

BY
John C. S. Chang
Acurex Corporation
P. O. Box 13109
Research Triangle Park, NC 27709

Norman Kaplan and Theodore G. Brna
U. S. Environmental Protection Agency
Industrial Environmental Research Laboratory
Research Triangle Park, NC 27711

ABSTRACT

Pilot plant tests have been conducted to evaluate the effects of magnesium and chloride ions on system performance of limestone-regenerated dual alkali processes under closed-loop operating conditions. It was found that limestone reactivity and solids dewatering properties are very sensitive to magnesium ion concentrations. The total magnesium ion concentration should be maintained below 1000 ppm for satisfactory performance under normal operation. A model which assumes competitive surface adsorption of calcium and magnesium ions was used to interpret the data. Limestone reactivity and solids dewatering properties decreased with the increase of chloride ion concentration. However, the effect of chloride ion accumulation was not significant until the concentration reached 80,000 ppm.

INTRODUCTION

Sodium-based dual alkali (DA) flue gas desulfurization (FGD) processes have the features of clear solution scrubbing, high SO_2 removal efficiency, low liquid-to-gas (L/G) ratio and high reliability[1]. Recent testing has demonstrated the feasibility of using limestone instead of lime for scrubbing liquor regeneration which makes DA processes more competitive with slurry scrubbing processes[2].

Since the limestone DA process uses concentrated sodium sulfite solution as the absorbent for SO_2 removal, closed water loops are desired to minimize the sodium makeup requirements. However, the closed-loop operation (i.e., the only water leaving the FGD system is through evaporation and filter cake moisture) also promotes the buildup of soluble salts in the recirculating scrubbing liquor. The primary sources of soluble salts include makeup water, reagents, and flue gas. Previous findings indicate that the accumulation of soluble salts, especially chloride ions, can have significant effects on system chemistry and scrubber performance of lime/limestone slurry FGD processes[3,4]. The most significant effects observed include decreases of equilibrium pH, SO_2 removal efficiency, and solids settling rate, and increase in gypsum scaling potential.

In order to broaden the data base of the limestone DA process and to evaluate the impacts of closed-loop operation, a series of pilot plant tests was conducted under the sponsorship of U.S. Environmental Protection Agency's (EPA) Industrial Environmental Research Laboratory in Research Triangle Park, NC (IERL-RTP). The testing concentrated on evaluating the effects of magnesium and chloride ions since appreciable accumulations of soluble salts containing these two species are expected in a limestone DA system under closed-loop operating conditions.

The current trend in power plant design is to use plant waste water (e.g., cooling tower blowdown) for FGD system makeup. Magnesium and chloride are the primary ingredients of soluble salts which enter the FGD system with plant waste water. Additional chloride ions may enter the scrubbing liquor through the absorption of HCl produced during the coal combustion process. In addition to makeup water, limestone is also an important source of magnesium ions. If closed-loop operation is used, the dissolved salts from either of the above sources can be concentrated to levels which are considerably higher than those presently observed in most systems. This paper summarizes selected results from the pilot plant study of the limestone DA process with total magnesium ion concentration up to 2000 ppm and chloride ion concentration to 150,000 ppm.

TEST FACILITIES

The IERL-RTP pilot facilities include a three-stage tray tower with 7.5 m^3/min (approximately 0.1 MW) flue gas capacity (Figure 1). The flue gas is drawn from a gas-fired boiler (no flyash is present). Pure SO_2 is injected to achieve the desired concentration in the flue gas. Regeneration of spent scrubbing liquor is performed in the four-tank-in-series reactor train with a total residence time of 80 minutes. Limestone is fed to the first reactor as 45% slurry. The feed rate is manually set as required for either pH or reactant stoichiometry control. Soda ash is added to the fourth reactor as sodium makeup. Reactor effluent slurry flows by gravity to the thickener centerwell. Clarified liquor overflows from thickener to the forward feed hold tank from which it is pumped to the tray tower. A horizontal belt filter is used for further dewatering of the thickener underflow solids.

Ultraviolet spectrophotometry (DuPont 400 SO_2 analyzer) was used to monitor the gas phase SO_2 concentrations and SO_2 removal efficiencies. The pH of scrubbing liquor in each reactor was measured hourly during pilot testing. Solid dewatering properties were characterized by hold tank slurry settling rate and filter cake insoluble solids concentration. Detailed descriptions of the test facilities and analytical procedures were reported earlier[5].

EFFECTS OF MAGNESIUM IONS

For the study of magnesium ion (Mg^{2+}) effects on the system performance of limestone dual alkali process, epsom salt ($MgSO_4 \cdot 5H_2O$) was added to adjust the Mg^{2+} concentration in the scrubbing liquor. The base case system performance was established without the addition of epsom salt; the steady-state concentration of Mg^{2+} was 355 ppm. In subsequent tests, all operating conditions -- except for Mg^{2+} concentration --were maintained constant; the concentration of Mg^{2+} was gradually increased by epsom salt addition to the first reactor. The maximum total Mg^{2+} concentration reached during this test series was 2000 ppm. The principal results of these tests are listed in Table 1. Summaries of liquor and solid analyses are listed in Tables 2 and 3.

Effects of 1000 ppm Mg^{2+}

A comparison of results obtained from run MG-1 with those from MG-2 indicated that the most significant change observed with the increase of total Mg^{2+} concentration up to 1000 ppm is the deterioration of solids dewatering properties as reflected by the decrease of insoluble solids in the filter cake. The base case (run MG-1) filter cake contained 52% solids; however, only 45% solids was obtained in the filter cake generated at 1000 ppm total Mg^{2+} concentration.

No magnesium sulfate was added to the system for run MG-3. The objective of this run was to evaluate the system performance with decreasing Mg^{2+} concentration. The mass balance indicated that the total Mg^{2+} concentration should drift down to

below 500 ppm. During the run, the total Mg^{2+} concentration decreased from 1000 ppm to about 625 ppm toward its end. A leak was discovered at the scrubber bleed/quench recirculation pump inlet which introduced air into the process stream and therefore caused high oxidation. The high oxidation, as confirmed by solids analysis results in Table 3, was reflected by increases of the sulfate-to-sulfite ratio to above 2.5. After the air leak problem was corrected, the sulfate-to-sulfite ratio decreased, but the test average was 2.4.

Very stable operation was maintained for run MG-4 without magnesium sulfate addition with the total Mg^{2+} concentration stabilizing at about 350 ppm. The sulfate-to-sulfite ratio decreased to 2.0, the filter cake insoluble solids reached 53%, and the slurry settling rate was 2.0 cm/min. The results confirmed the base case solids quality and scrubber performance obtained from run MG-1.

Effects of 2000 ppm Mg^{2+}

Epsom salt was then added to the first reactor to raise the Mg^{2+} concentration for run MG-5. No significant changes of system performance were observed except the deterioration of filter cake quality when the total Mg^{2+} concentration reached 1000 ppm. The filter cake insoluble solids dropped from 53% to 47% at 1000 ppm total Mg^{2+} concentration and confirmed the results observed during runs MG-1 and MG-2. However, a further increase of the Mg^{2+} concentration caused significant changes in system performance. When the total Mg^{2+} concentration exceeded 1500 ppm, pH decreases were observed throughout the system. The SO_2 removal efficiency also decreased. Filter cake quality deteriorated further to below 40% insoluble solids. The solids settling rate also began to drop. At 2000 ppm total Mg^{2+} concentration, a system upset with non-settling solids occurred. The solids settling rate dropped to below 0.1 cm/min, while only 28% insoluble solids were obtained from the filter cake. The pH of the regenerated liquor was 6.2 (base case pH was 6.6) and SO_2 removal efficiency was 85% (base case removal efficiency was 92%). The solids content of slurries in the reactors reached 4.7% (base case solids content was 2.1%) due to the solids carryover in the thickener overflow.

Results of Chemical Analysis

Several sets of samples were taken from each reactor and hold tank for liquid and solids analyses to characterize the system chemistry at various Mg^{2+} concentrations. Results of the chemical analyses are shown in Figures 2 to 8. Figure 2 shows the profile of total Mg^{2+} concentration across the pilot plant system. A slight drop of Mg^{2+} concentration was observed from the scrubber bleed hold tank (V-102) to the first reactor (V-105), especially for the high Mg^{2+} concentration runs. The concentration drop was not very significant since the changes were within ± 5% (the range of experimental error). However, a magnesium loss across the reactors is implied. Magnesium lost in this manner is probably coprecipitated with calcium sulfite/sulfate.

The pH profile is shown in Figure 3. A significant drop in the system pH was obtained when the total Mg^{2+} concentration was increased from 1000 to 2000 ppm. The scrubber bleed hold tank pH decreased from 6.3 to 5.6 and the forward feed hold tank pH also decreased from 6.7 to 6.2. However, the increase of pH across the reactors was observed even at 2000 ppm total Mg^{2+} concentration, indicating that the limestone dissolution was not completely stopped by increasing the Mg^{2+} concentration.

The total oxidizable sulfur (TOS) and sulfate ion concentrations are shown in Figures 4 and 5, respectively. Similar concentration levels and concentration trends were observed for both species at the three Mg^{2+} concentrations tested. Figures 4 and 5 confirm that the concentrations of important species, such as TOS and sulfate ion, were not altered by increasing the Mg^{2+} concentration by epsom salt addition.

Figure 6 shows the total alkalinity concentrations across the system. Since the TOS concentrations were maintained at about the same levels for all runs (Figure 4), the decrease of total alkalinity when total Mg^{2+} concentration was increased from 1000 to 2000 ppm reflects the pH drop caused by the increase of magnesium ion concentrations.

The calcium ion (Ca^{2+}) and total carbonate concentrations are shown in Figures 7 and 8, respectively. The concentration levels and the trends of Ca^{2+} and total carbonate profiles obtained at the three Mg^{2+} concentrations are very similar.

Solids Analysis

The product solids obtained at various magnesium ion concentrations were examined under a scanning electron microscope (SEM) to observe the detailed morphology of the individual solid particles. As can be seen in the SEM photomicrographs reproduced in Figures 9 through 12, the product solids were physically different. Figure 9 shows the solids taken at the base case conditions where the particles gave a 50 to 55% solids filter cake with agglomerates of well-defined platelets. The thickness of each platelet can be seen clearly in Figure 9b which was taken at a magnification of 5000x.

Photomicrographs of solids produced at the 1000 ppm total Mg^{2+} concentration are shown in Figure 10. Compared with the base case solids (Figure 9), the solid particles in Figure 10 were composed of thinner, smaller platelets. This was reflected in poorer filter cake qualities (45 to 50% insoluble solids).

Photomicrographs of solids produced at 2000 ppm total Mg^{2+} concentration are shown in Figure 11 which indicates the solid particles are composed of ill-defined, needle-like platelets. Furthermore, Figure 11b reveals serious crystal defects. The poor crystal properties were evidenced by an extremely low settling rate (less than 0.1 cm/min) and very few filter cake insoluble solids (less than 30%).

In summary, two significant effects of Mg^{2+} concentration on DA system performance were observed. First, the pilot plant data indicated that the solid product dewatering properties are very sensitive to Mg^{2+} concentration. Photomicrographs show that the deterioration of solids dewatering properties is caused by crystal morphology changes comprising crystal size decreases and crystal defects. Second, the limestone dissolution rate decreased as reflected by the system pH drop. This effect is not very significant until the total Mg^{2+} concentration reaches about 1000 ppm.

Surface Adsorption Model

The effect of Mg^{2+} on the dissolution rate of $CaCO_3$ has been investigated with a pH-stat laboratory experiment[6]. The results indicated that the presence of Mg^{2+} in the solution reduces the $CaCO_3$ dissolution rate. To interpret the data, it was assumed that Mg^{2+} can be adsorbed on the surface of $CaCO_3$ particles to form a surface Ca-Mg-carbonate. The adsorption reduces the dissolution rate since the surface is partially blinded by adsorbed Mg^{2+}. It was also assumed that the reduction of the dissolution rate is proportional to the fraction of the surface (θ) occupied by the adsorbed Mg^{2+}, which can be expressed by the Langmiur adsorption isotherm:

$$\theta = ac/(1 + bc) \qquad (1)$$

where a and b are constants and c is the concentration of adsorbed species.

The dissolution rate (R) can be determined from:

$$R = kA\,(1 - r^{1/2})^n \qquad (2)$$

where k is the apparent rate constant, A is the active surface area, r is the degree of $CaCO_3$ saturation, and n is a constant. In the presence of Mg^{2+}, the active surface area A is related to θ by:

$$A = (1 - \theta) \qquad (3)$$

The inhibition effect of Mg^{2+} on $CaCO_3$ dissolution rate can be described by the following correlation derived from Equations 1, 2 and 3.

$$(1 - R/R_o) = 1.38 \times 10^5\,[Mg^{2+}]/(1 + 1.68 \times 10^5\,[Mg^{2+}]) \qquad (4)$$

where R_o is the dissolution rate in the absence of Mg^{2+} and $[Mg^{2+}]$ is the concentration of total magnesium in moles cm^{-3}.

In wet flue gas desulfurization processes, either dual alkali or limestone slurry, the combined effects of calcium and magnesium actually determine the limestone dissolution rate. Sjoberg's results[6] indicated that Ca^{2+} can inhibit $CaCO_3$ dissolution rate much more effectively than Mg^{2+} by the same surface adsorption phenomenon. The combined effects of Ca^{2+} and Mg^{2+} can be described as competitive adsorption, and the limestone surface will act as an ion-exchanger. The fraction of surface occupied by adsorbed Ca^{2+} and Mg^{2+} can be expressed as:

$$\theta = \theta_{Ca} + \theta_{Mg} = \sum_{i=1}^{n} a_i c_i \,/\, (1 + \sum_{i=1}^{n} b_i c_i) \qquad (5)$$

where a_i and b_i are constants and c_i is the concentration of the adsorbed species i. The reduction of dissolution rate is proportional to θ, or:

$$(1 - R/Ro) \propto \theta \qquad (6)$$

In the ideal case, a_i and b_i are constants independent of c_i. Therefore,

$$\frac{\theta_{Mg}}{\theta_{Ca}} = K' \frac{[Mg^{2+}]}{[Ca^{2+}]} \qquad (7)$$

where K' is a constant with a value of 0.033 as obtained by Sjoberg[6].

Equation (7) indicates that the relative effectiveness of Mg^{2+} and Ca^{2+} in inhibiting the limestone dissolution rate depends on the ratio of Mg^{2+} concentration to Ca^{2+} concentration. On the other hand, the sensitivity of limestone dissolution rate to the Mg^{2+} concentration is determined by the Ca^{2+} concentration. As indicated by Equation (7), when the minimum ratio (θ_{Mg}/θ_{Ca}) of 0.5 is required for Mg^{2+} to effectively inhibit limestone dissolution rate, dual alkali processes need only 908 ppm Mg^{2+} since the normal Ca^{2+} concentration in the first reactor is about 100 ppm. Furthermore, if competitive adsorption of Mg^{2+} and Ca^{2+} also occurred on the $CaSO_3$ surface, the adsorbed Mg^{2+} can act as an impurity which causes crystal defects and inhibits crystal growth. As a result, the properties of the solid product deteriorate with the increase of Mg^{2+} concentration as reflected by the decrease of slurry settling rate and filter cake insoluble solids obtained from pilot plant testing.

EFFECTS OF CHLORIDE IONS

Chloride ions (Cl^-) accumulating in the scrubbing liquor will be balanced by cations such as sodium (Na^+) and Mg^{2+}. Since previous data indicated that high magnesium ion concentrations are not desirable, it is expected that Na^+ will be the cation associated with the Cl^- in limestone dual alkali scrubbing solutions.

The pilot evaluation test was started on the base case (no chloride addition) conditions with 183 ppm Cl^- concentration. Industrial grade sodium chloride was then added to the third reactor to raise the Cl^- concentration to 20,000, 50,000, and 80,000 ppm, respectively. The principal results of these tests are listed in Table 4. Summaries of liquor and solids analyses are listed in Tables 5 and 6. The most significant change observed with the increase of Cl^- concentration was the decrease of system pH. While all the other variables (limestone feed rate, SO_2 feed rate, active sodium concentration, sulfate-to-sulfite ratio, etc.) were maintained at approximately constant levels, the pH of regenerated liquor decreased from 6.6 to 6.5, 6.3, and 6.2 as the Cl^- concentration increased from the base case to 20,000, 50,000, and 80,000 ppm, respectively. Correspondingly, the SO_2 removal efficiency also dropped slightly from 93 to 92, 91, and 90%, respectively. In order to maintain constant total alkalinity concentrations, the soda ash make-up rate was increased by more than 50%. No significant changes in solids quality were observed with the increase of Cl^- concentration when the Cl^- concentration was below 80,000 ppm. The filter cake insoluble solids content fluctuated between 50 and 55% and the sulfate-to-sulfite ratio dropped slightly from 1.9 to 1.8. Filter cake analyses indicated that the overall oxidation decreased from 6.9% to 4.0% as the Cl^- concentration increased from the base case level to 80,000 ppm.

Chloride ion concentrations of 100,000 ppm and 150,000 ppm were also tested. Corresponding to these Cl^- concentrations, the Na^+ concentrations reached 116,900 ppm and 140,500 ppm, respectively. As observed in previous runs, the system pH dropped with the increase of Cl^- concentration. The base case (no chloride addition) regenerated liquor pH was 6.7. At 100,000 ppm Cl^- concentration, the regenerated liquor pH fell to 6.1. The regenerated liquor pH further decreased to 5.9 when the Cl^- concentration was increased to 150,000 ppm.

The most significant operating problem encountered during runs with 100,000 and 150,000 ppm Cl^- was scaling in the absorber. The quench nozzle scaled and plugged, and a very high pressure drop (over 10 in. H_2O) across the absorber was obtained. Layers of hard scale composed of $CaSO_3/SO_4$ were found on the absorber walls. A large quantity of water soluble sodium scale was deposited beneath the middle and the bottom trays. Neither scale contained significant amounts of chloride.

In addition to scaling, system performance also deteriorated. Only 86% SO_2 removal efficiency was obtained at 150,000 ppm chloride, significantly lower than the 93% at base case conditions. Filter cake insoluble solids also decreased to 39% compared with 50 to 55% for the base case. Decreases of TOS and total alkalinity concentrations were observed and reflected the increased liquor loss and sodium consumption.

SUMMARY

In summary, the pilot plant data indicate that:

- The solid product dewatering properties are very sensitive to Mg^{2+} concentration. Significant drops (5% or more) of filter cake insoluble solid concentrations were obtained with the increase of total Mg^{2+} concentration from 500 ppm to 1000 ppm. Solids quality deteriorated rapidly after the

total magnesium ion concentration exceeded 1000 ppm. At a total Mg^{2+} concentration of 2000 ppm, a system upset with non-settling solids occurred. The solids settling rate dropped below 0.1 cm/min, and only 28% insoluble solids were obtained from the filter cake. Scanning electron micrographs showed that the deterioration of solids dewatering properties was caused by crystal morphology changes reflecting crystal size decreases and crystal defects.

- The limestone dissolution rate decreased as shown by decreasing system pH with increasing Mg^{2+} concentration. This effect is relatively small until the total magnesium ion concentrations reach about 1000 ppm.

- The effect of Mg^{2+} concentration on limestone dissolution rate can be explained by a surface adsorption model. The adsorption of Mg^{2+} reduces the limestone dissolution rate because the surface is partially blinded by the adsorbed magnesium ions. The competitive adsorption of calcium and magnesium ions was described by a mathematical model based on the Langmuir adsorption isotherm. The model was used to explain the sensitivity of limestone dissolution rate to magnesium ion concentration under limestone dual alkali operating conditions.

- When the chloride ion concentration is below 80,000 ppm, the most significant change observed with the increase of Cl^- concentration was the decrease of system pH. Correspondingly, slight drops of SO_2 removal efficiency were also obtained.

- When the chloride ion concentration is above 100,000 ppm, system performance deteriorated with the increase of chloride ion concentration. In addition to the decreasing scrubbing solution pH and SO_2 removal efficiency, the filter cake insoluble solids also decreased and resulted in increased liquor losses and sodium consumptions.

REFERENCES

1. Kaplan, N., "Summary of Utility Dual Alkali Systems," Proceedings: EPA Flue Gas Desulfurization Symposium (Las Vegas, March 1979), Volume 2, EPA-600/7-79-1676, July, 1979.

2. Chang, J. C. and N. Kaplan, "Pilot Evaluation of Limestone Regenerated Dual Alkali Process," presented at the 8th EPA/EPRI Flue Gas Desulfurization Symposium, New Orleans, LA, November, 1983.

3. Chang, J. C., "Pilot Plant Tests of Chloride Ion Effects on Wet FGD System Performance," EPA-600/15-7-84-039, May 1984.

4. Laslo, D., J. C. Chang, and J. D. Mobley, "Pilot Plant Tests on the Effects of Dissolved Salts on Lime/Limestone FGD Chemistry," Presented at the 8th EPA/EPRI Flue Gas Desulfurization Symposium, New Orleans, LA, November, 1983.

5. Chang, J. C., J. H. Dempsey, and N. Kaplan, "Pilot Testing of Limestone Regeneration in Dual Alkali Processes," Proceedings: Symposium on Flue Gas Desulfurization," EPRI CS-2897, March, 1983.

6. Sjoberg, E. L., "Kinetics and Mechanism of Calcite Dissolution in Aqueous Solutions at Low Temperatures," Stockholm Contributions in Geology, 32(1), 1981.

TABLE 1. MAGNESIUM-ION-EFFECT TEST CONDITIONS

Run	MG-1	MG-2	MG-3	MG-4	MG-5
Mg^{2+} concentration, ppm	355	1060	625	356	2000
Tower pressure drop, in. H_2O	8.1	8.4	7.9	7.8	8.2
Liquor forward feed, gpm	1.4	1.4	1.4	1.4	1.4
Scrubber feed pH	6.6	6.6	6.6	6.6	6.2
Scrubber effluent pH	6.2	6.2	6.2	6.2	5.6
Inlet SO_2 concentration, ppm	3010	2990	2990	3050	3020
SO_2 feed rate, lb/hr	6.7	6.7	6.6	6.7	6.6
SO_2 absorption, wt. %	92.7	91.8	91.0	92	85
SO_2 make-per-pass, mmol/l	139	137	132	138	125
Limestone slurry feed rate, lb/hr	23	23	22	22	22
Limestone slurry solids, wt. %	45	45	45	45	45
Flue gas O_2, vol. %	6.4	7.0	6.1	6.9	7.2
Thickener solids, wt. %	19	18	16	20.1	7.8
Filter cake solids, wt. % (insoluble)	52	45	48	53	28
Filter wash rate (nominal), gph	3	3	3	3	3
Na concentration, g/l	57	55.6	57.4	54.0	49.7
TOS, gmol/l	0.72	0.67	0.70	0.74	0.67
Ca concentration, ppm	88	52	74	62	58
Total alkalinity, gmol/l (V-113)	0.42	0.41	0.38	0.42	0.28
Na in filter cake, mg/g[a]	15.5	18.6	16.9	12.6	(d)
Run time, hours	81	78	85	92	67
Limestone stoichiometry[b]	1.07	1.08	1.06	1.03	1.13
Settling rate (reactor), cm/min	2.0	1.9	2.2	2.2	<0.1
Settling test % solids	2.1	2.1	2.6	2.1	4.7
Active Na, gmol/l[c]	1.14	1.08	1.08	1.16	0.95
SO_4/sulfite	2.05	2.15	2.4	2.0	3.2

(a) Washed in the belt filter
(b) Mass balance
(c) Active Na = TOS + Total Alkalinity, gmol/l
(d) Data not available

TABLE 2. SUMMARY OF THICKENER LIQUOR ANALYSIS FROM MAGNESIUM-ION-EFFECT TESTS

Run No.	MG-1	MG-2	MG-3	MG-4	MG-5
Component, g/l					
Ca	0.088	0.052	0.074	0.062	0.058
Mg	0.355	1.06	0.625	0.356	2.02
Na	57.0	55.6	57.4	54.0	49.7
TOS as SO_3	57.6	53.6	55.6	59.3	53.6
SO_4	82.6	84.5	86.4	80.6	86.4
CO_3	2.73	2.54	2.35	2.1	2.03
Cl^-	0.165	0.174	0.192	0.182	0.175
pH	6.7	6.7	6.6	6.7	6.2

TABLE 3. SUMMARY OF FILTER CAKE ANALYSIS FROM MAGNESIUM-ION-EFFECT TESTS

Run No.	MG-1	MG-2	MG-3	MG-4	MG-5
Component, mg/g					
Total S as SO_3	529	522	525	509	511
TOS as SO_2	379	378	363	382	376
Carbonate as CO_2	42	47	43	42	56
Ca	294	297	298	296	298
Mg	2.6	3.4	2.8	2.5	3.6
Na	5.7	5.8	5.8	4.4	5.3
Oxidation, %	10.4	9.5	13.6	6.2	8.0
L/S Utilization, %(a)	89.9	87.8	88.1	86.0	85.7

(a) SO_3/Ca
(b) data not available

TABLE 4. CHLORIDE-ION-EFFECT TEST CONDITIONS

Run No.	CL-1	CL-2	CL-3	CL-4	CL-5	CL-6
Cl^- concentration, ppm	Base Case	20000	50000	80000	100000	150000
Tower pressure drop, in. H_2O	8.0	8.1	8.1	8.2	8.9	10.2
Liquor forward feed, gpm	1.4	1.4	-(d)	1.4	1.4	1.4
Scrubber feed pH	6.6	6.5	6.3	6.2	6.1	5.9
Scrubber effluent pH	6.2	6.1	5.9	5.8	5.7	5.5
Inlet SO_2 concentration, ppm	3040	3010	3060	3010	3030	3010
SO_2 feed rate, lb/hr	6.6	6.7	6.7	6.6	6.6	6.7
SO_2 absorption, %	93	92	91	90	89	86
SO_2 make-per-pass, mmol/l	137.1	137.7	-	122.7	131	129
Limestone slurry feed rate, lb/hr	22	22	22	22	22	22
Limestone slurry solids, wt. %	45	45	45	45	45	45
Flue gas O_2, vol. %	5.6	5.1	5.3	4.7	5.2	5.1
Thickener solids, wt. %	22.8	19.8	23.4	22.1	18.1	20.2
Filter cake solids, wt. % (insoluble)	53	52	51	52	48	39
Filter wash rate (nominal), gph	3	3	3	3	3	3
Na concentration, g/l	47.8	59.6	78.8	96.9	116.9	140.5
TOS, gmol/l	0.70	0.65	0.66	0.64	0.61	0.47
Ca concentration, ppm	61	57	58	49	51	36
Total alkalinity, gmol/l (V-113)	0.44	0.41	0.40	0.39	0.34	0.29
Na in filter cake, mg/g(a)	8.2	9.4	13.3	14.6	17.7	24.5
Run time, hours	85	62	68	58	84	72
Limestone stoichiometry(b)	1.03	1.03	1.04	1.07	1.08	1.10
Settling rate (reactor), cm/min	2.3	2.1	1.8	1.9	1.8	1.7
Settling test % solids	2.0	1.9	2.7	1.8	2.1	2.4
Active Na, gmol/l(c)	1.14	1.06	1.06	1.03	0.95	0.76
SO_4/Sulfite	1.9	1.9	1.8	1.8	1.84	1.72

(a) Washed in the belt filter
(b) Mass balance
(c) Active Na = TOS + Total Alkalinity, gmol/l
(d) Flowmeter not operational

TABLE 5. SUMMARY OF THICKENER LIQUOR ANALYSIS FROM CHLORIDE-ION-EFFECT TESTS

Run No.	CL-1	CL-2	CL-3	CL-4	CL-5	CL-6
Component, g/l						
Ca	0.061	0.057	0.058	0.049	0.051	0.036
Mg	0.344	0.298	0.333	0.247	0.176	0.072
Na	47.8	59.6	78.8	96.9	116.9	140.5
TOS as SO_3	56.0	52.0	52.8	51.2	48.6	37.6
SO_4	80.3	76.2	69.1	67.3	60.2	48.0
CO_3	2.68	2.25	2.12	1.95	1.25	0.96
Cl	0.183	20.1	50.3	80.2	100.0	150.0
pH	6.6	6.5	6.3	6.2	6.1	5.9

TABLE 6. SUMMARY OF FILTER CAKE ANALYSIS FROM CHLORIDE-ION-EFFECT TESTS

Run No.	CL-1	CL-2	CL-3	CL-4	CL-5	CL-6
Component, mg/g						
Total S as SO_3	513	498	503	505	501	491
TOS as SO_2	382	372	381	388	383	372
Carbonate as CO_2	40	42	43	46	56	61
Ca	295	286	292	298	308	307
Mg	2.4	2.3	2.4	3.2	3.0	2.6
Na	5.9	(b)	6.2	5.8	6.5	5.9
Oxidation, %	6.9	6.6	5.3	4.0	4.4	5.3
L/S Utilization, %(a)	86.9	87.1	86.1	84.7	81.3	80.0

(a)SO_3/Ca
(b)data not available

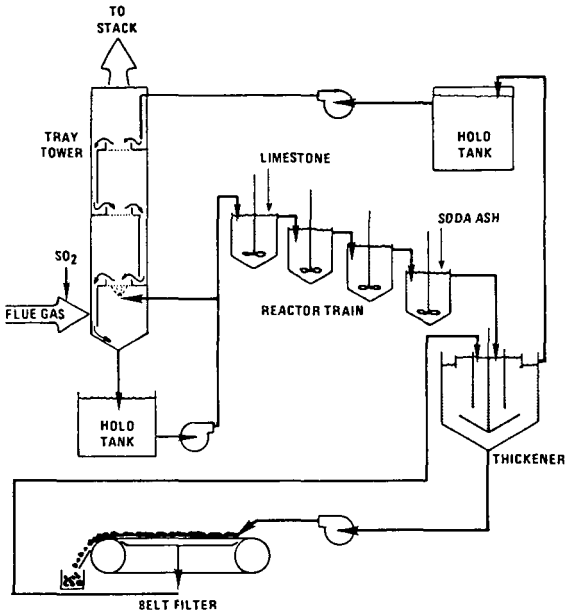

Figure 1. Flow diagram of IERL-RTP dual alkali pilot plant.

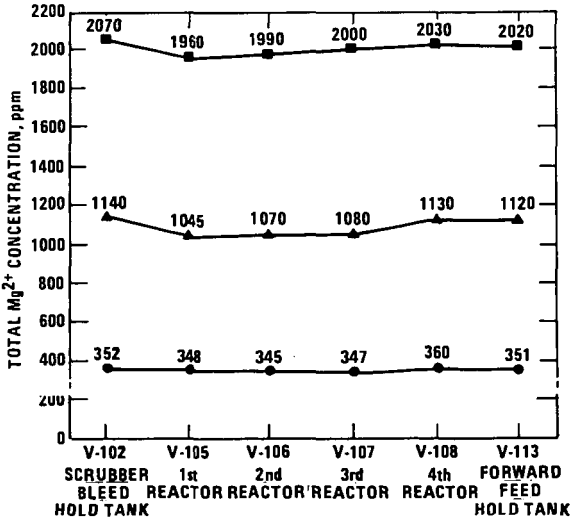

Figure 2. Distribution of magnesium ion concentration in limestone DA pilot plant.

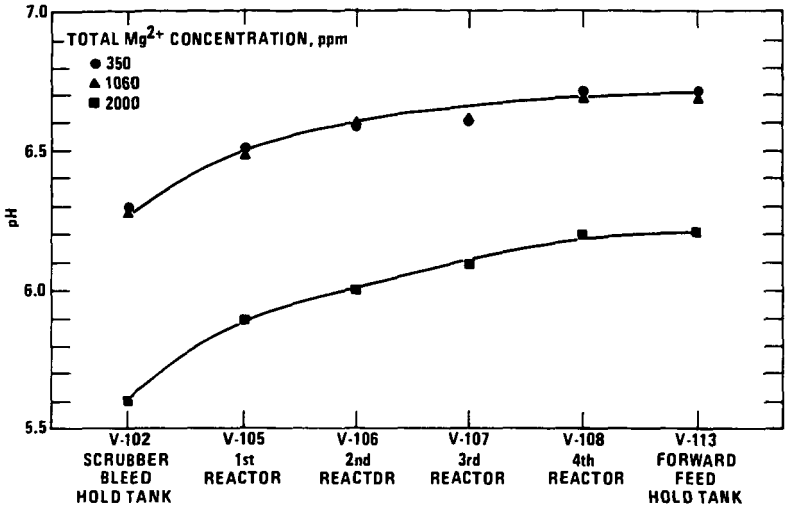

Figure 3. Profiles of pH values in limestone DA pilot plant.

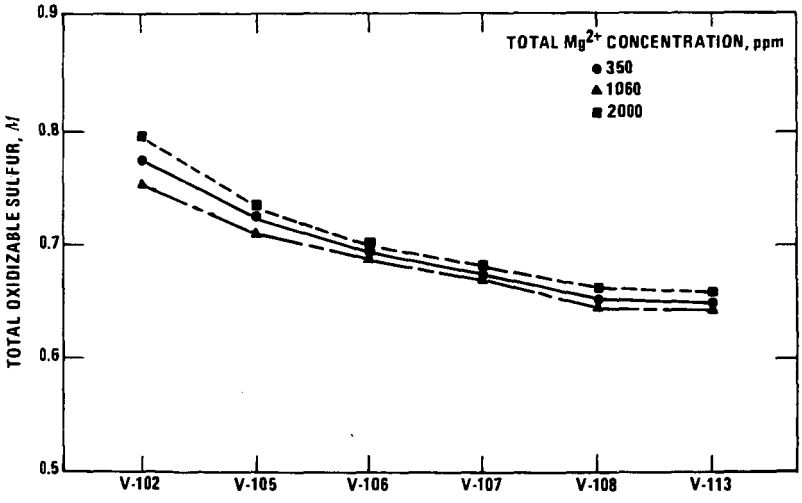

Figure 4. Total oxidizable sulfur concentrations in limestone DA pilot plant.

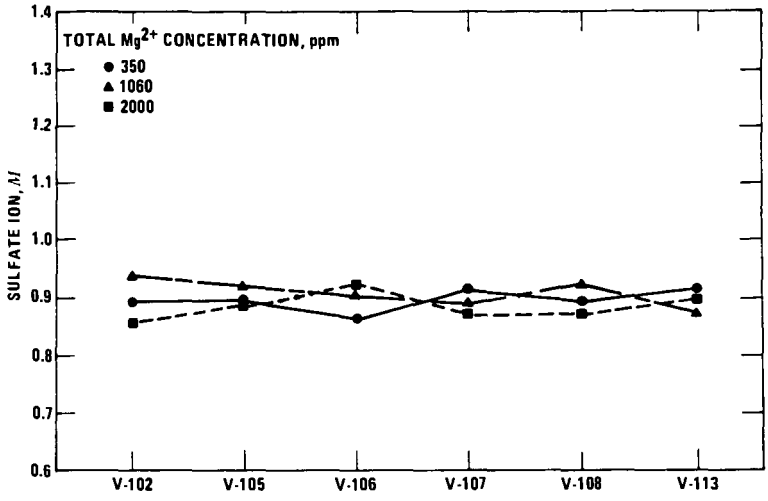

Figure 5. Distribution of sulfate ion concentration in limestone DA pilot plant.

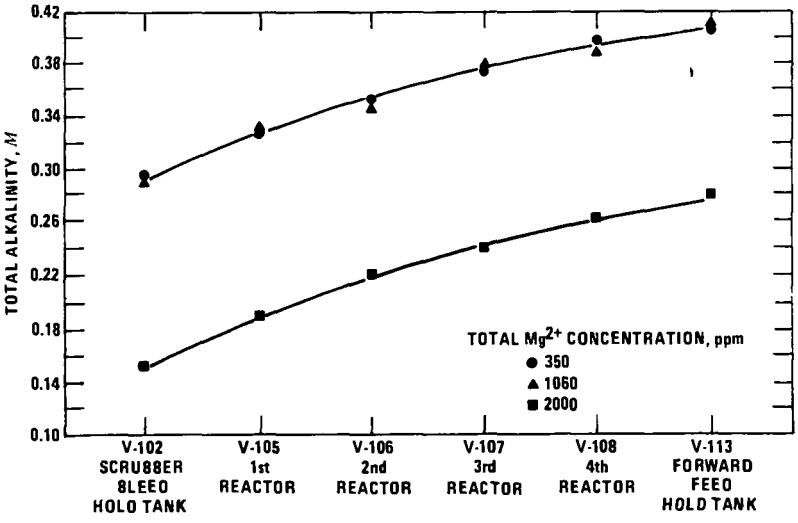

Figure 6. Total alkalinity concentrations in limestone DA pilot plant.

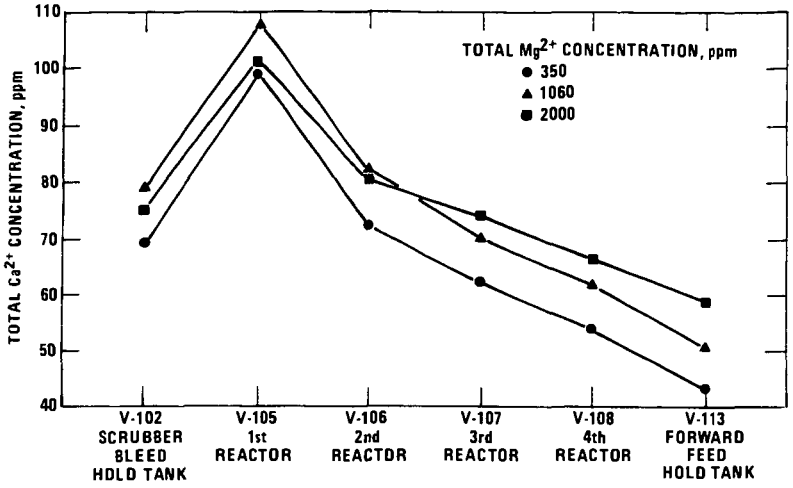

Figure 7. Distribution of total calcium ion concentration in limestone DA pilot plant.

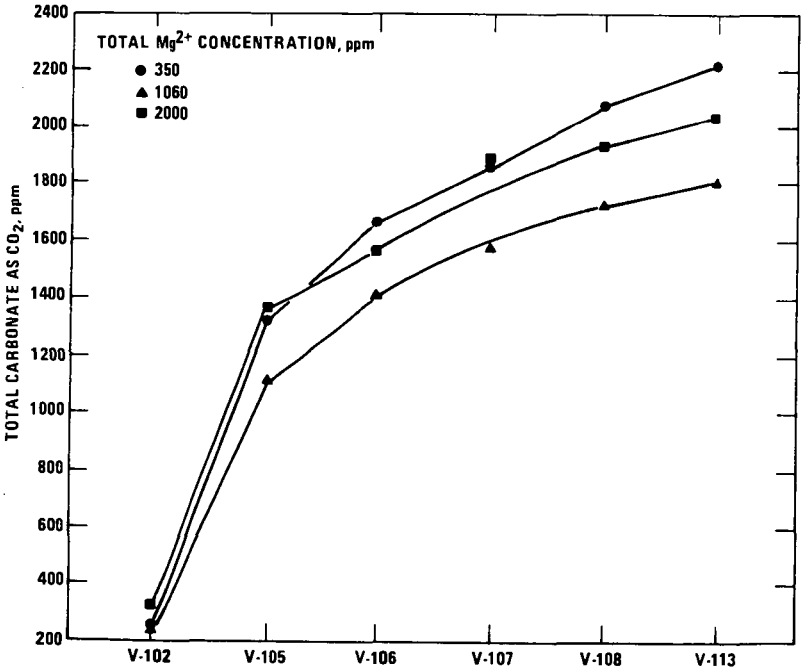

Figure 8. Distribution of carbonate ion concentration in limestone DA pilot plant.

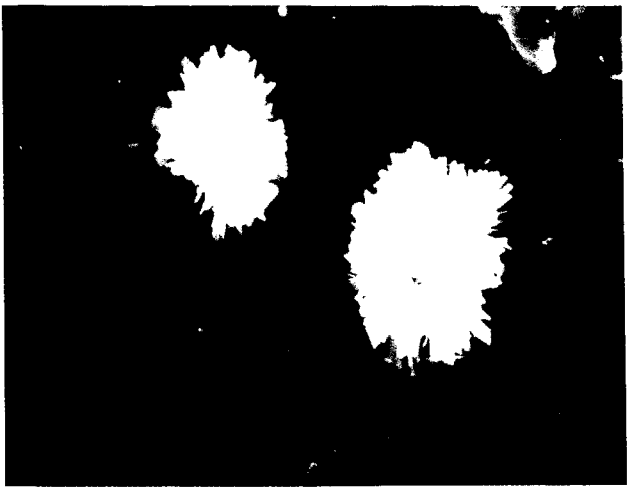

(a) 1000X

(b) 5000X

Figure 9. Scanning electron micrograph of base case solid products.

(a) 1000 X

(b) 5000 X

Figure 10. Scanning electron micrograph of solid products at 1000 ppm Mg^{2+} concentration.

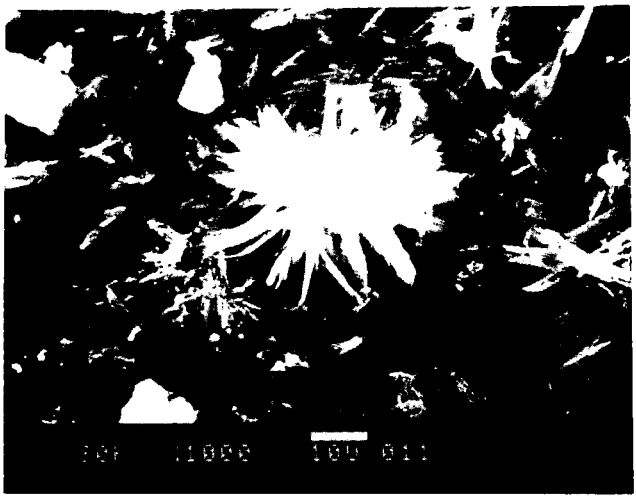

(a) 1000X

(b) 5000X

Figure 11. Scanning electron micrograph of solid products at 2000 ppm Mg^{2+} concentration.